Metabolism and proteomics of large and small dense LDL in combined hyperlipidemia: effects of rosuvastatin[1][s]

Nuntakorn Thongtang,[2,3,]* Margaret R. Diffenderfer,[2,]* Esther M. M. Ooi,[4,]* P. Hugh R. Barrett,[†] Scott M. Turner,[5,§] Ngoc-Anh Le,**[,††] W. Virgil Brown,**[,††] and Ernst J. Schaefer[6,]*

Cardiovascular Nutrition Laboratory, Jean Mayer USDA Human Nutrition Research Center on Aging at Tufts University,* Boston, MA; School of Biomedical Sciences, University of Western Australia,[†] Perth, Western Australia, Australia; KineMed, Inc.,[§] Emeryville, CA; Atlanta Veterans Affairs Medical Center,** Decatur, GA; and Emory University School of Medicine,[††] Atlanta, GA

Abstract   Small dense LDL (sdLDL) has been reported to be more atherogenic than large buoyant LDL (lbLDL). We examined the metabolism and protein composition of sdLDL and lbLDL in six subjects with combined hyperlipidemia on placebo and rosuvastatin 40 mg/day. ApoB-100 kinetics in triglyceride-rich lipoproteins (TRLs), lbLDL (density [d] = 1.019–1.044 g/ml), and sdLDL (d = 1.044–1.063 g/ml) were determined in the fed state by using stable isotope tracers, mass spectrometry, and compartmental modeling. Compared with placebo, rosuvastatin decreased LDL cholesterol and apoB-100 levels in TRL, lbLDL, and sdLDL by significantly increasing the fractional catabolic rate of apoB-100 (TRL, +45%; lbLDL, +131%; and sdLDL, +97%), without a change in production. On placebo, 25% of TRL apoB-100 was catabolized directly, 37% was converted to lbLDL, and 38% went directly to sdLDL; rosuvastatin did not alter these distributions. During both phases, sdLDL apoB-100 was catabolized more slowly than lbLDL apoB-100 ($P < 0.01$). Proteomic analysis indicated that rosuvastatin decreased apoC-III and apoM content within the density range of lbLDL ($P < 0.05$). In our view, sdLDL is more atherogenic than lbLDL because of its longer plasma residence time, potentially resulting in more particle oxidation, modification, and reduction in size, with increased arterial wall uptake. Rosuvastatin enhances the catabolism of apoB-100 in both lbLDL and sdLDL.**—Thongtang, N., M. R. Diffenderfer, E. M. M. Ooi, P. H. R. Barrett, S. M. Turner, N.-A. Le, W. V. Brown, and E. J. Schaefer. **Metabolism and proteomics of large and small dense LDL in combined hyperlipidemia: effects of rosuvastatin. *J. Lipid Res.* 2017. 58: 1315–1324.**

An elevated LDL cholesterol concentration is a primary risk factor for CVD, and lowering LDL cholesterol with statins has clearly been shown to decrease this risk (1). LDL consists of particles of varying size, density, and composition, as assessed by ultracentrifugation, gradient gel electrophoresis, NMR, and ion mobility (2). In 2010, Krauss concluded that there was "as yet inconclusive evidence as to the extent to which LDL and HDL subfraction measurements improve clinical assessment of CVD risk beyond standard lipid risk markers" (2). Recently, measurements of small dense LDL [sdLDL; density (d) = 1.044–1.063 g/ml] cholesterol in the Framingham Offspring Study, the Multi-Ethnic Study of Atherosclerosis (MESA), and the Atherosclerosis Risk in Communities (ARIC) Study, by using an automated assay developed by Hirano et al. (3), have demonstrated that sdLDL cholesterol is a significantly better marker of coronary heart disease risk than LDL cholesterol

(4–6). The assay separated sdLDL from large buoyant LDL (lbLDL; d = 1.019–1.044 g/ml) by using surfactants and sphingomyelinase; measured the cholesterol content of LDL particles 15–20 nm in diameter, corresponding to the density range of 1.044–1.063 g/ml; and had a coefficient of variation of <5%. In contrast, previous methods of LDL subfractionation, such as ultracentrifugation, gradient gel electrophoresis, NMR, and ion mobility, differentiated LDL particles based on their density, size, and charge (7–10). Lack of particle standardization and reproducibility among the LDL subfractions assayed by these earlier methods has led to a wide range of variation (6–93%) among the results. The new automated homogeneous assay based on direct precipitation methods and the measurement of cholesterol has led to significantly improved measurement reliability (3–6, 11).

We have documented previously that high-intensity statin therapy with either atorvastatin 80 mg/day or rosuvastatin 40 mg/day significantly lowers not only total LDL cholesterol, but also sdLDL cholesterol by approximately 50% (12). High-intensity statin therapy has been recommended for patients with established CVD by the recent American College of Cardiology/American Heart Association guidelines panel (13). Both atorvastatin and rosuvastatin at maximal doses lower LDL apoB concentrations, primarily by enhancing apoB catabolism (14–16). Our goal in this study, therefore, was to examine the metabolism of apoB-100 within lbLDL and sdLDL in subjects with combined hyperlipidemia in the nonfasting state and to compare the effects of intensive statin therapy on these processes, relative to placebo.

Proteomic analysis has found significant differences in the proteome of LDLs compared with that of apoB-containing lipoproteins in a lower density range (17–19). The differences suggest that LDL particles acquire some proteins directly from plasma, HDL particles, or peripheral cells, and not just from the lipolysis of triglyceride-rich lipoproteins (TRLs; d < 1.019 g/ml). It is possible that some of these proteins have LDL-specific functions that might alter the metabolism of LDL subfractions and provide an explanation for the increased atherogenicity of sdLDLs relative to lbLDLs. Therefore, an additional objective was to examine the protein composition of lbLDL and sdLDL particles in the study subjects while on placebo and maximal-dose rosuvastatin therapy. We chose to separate the two LDL fractions by ultracentrifugation at d = 1.044 g/ml so that sdLDL would be defined as it was in the Framingham Offspring Study, MESA, and ARIC (4–6).

MATERIALS AND METHODS

Subjects

Six subjects (three men and three postmenopausal women; ages 63 ± 5 years, mean ± SEM; BMI, 25.5 ± 1.5 kg/m^2) with combined hyperlipidemia, who were enrolled in a larger apolipoprotein metabolic study (16), participated in this study. Plasma lipid criteria for enrollment were as follows: triglyceride (TG) levels ⩾ 1.69 mmol/l, LDL cholesterol levels ⩾ 3.62 mmol/l, and HDL cholesterol levels < 1.29 mmol/l. Subjects with LDL cholesterol levels ⩾ 3.62 mmol/l with or without cholesterol-lowering medication, with documented T2D controlled with diet or oral antidiabetic agents, or with hypertension under stable management were eligible to participate. Subjects on a cholesterol-lowering regimen at the time of enrollment entered a 4–6 week washout period before starting the study. Exclusion criteria have been described previously in detail (16). All subjects met the lipid inclusion criteria at the beginning of the study: total cholesterol (TC), 5.93 ± 0.33 mmol/l; LDL cholesterol, 4.14 ± 0.42 mmol/l; HDL cholesterol, 1.11 ± 0.17 mmol/l; and TGs, 2.16 ± 0.57 mmol/l. There were no significant gender-attributable differences in these parameters.

The study protocol was approved by the Human Institutional Review Board of Emory University (Atlanta, GA), the Research and Development Committee at the Atlanta Veterans Affairs Medical Center (Decatur, GA), and the Human Institutional Review Board of Tufts Medical Center and Tufts University Health Sciences (Boston, MA). Written informed consent was obtained from each study subject. No serious adverse event was reported during the study. No clinical trial registration number was assigned to the protocol because enrollment of the subjects occurred before 2005 (16).

Study design

The larger metabolic study was a fixed-sequence, placebo-controlled, dose-titration, single-blind protocol intended to imitate the clinical management of statin therapy (16). All subjects, independent of prior cholesterol-lowering medication, were followed for three 8 week phases: placebo, rosuvastatin 5 mg/day, and rosuvastatin 40 mg/day. There was no washout period between the phases. The subjects were instructed to take two tablets every morning, i.e., two placebo tablets during the first phase; one rosuvastatin 5 mg tablet and one placebo tablet during the second phase; and two rosuvastatin 20 mg tablets during the third phase. In this subset assessment of apoB-100 metabolism in LDL subfractions, only samples from the placebo and rosuvastatin 40 mg/day phases were analyzed.

At the end of each 8 week treatment phase, the subjects were admitted to the Clinical Research Unit of the Atlanta Clinical and Translational Science Institute for a 69 h metabolic study, under fed conditions (16). After an overnight fast, the subjects received a bolus injection of 60 μmol/kg body weight [5,5,5-^{2}H] L-leucine (Cambridge Isotopes, Andover, MA) to determine the kinetics of apoB-100. Blood samples were collected into tubes containing EDTA (0.15%) at baseline (0 h, 8 AM) and at 30 min, 1, 2, 4, 6, 8, 10, 12, 14, 21, 27, 33, 45, 57, and 69 h after the isotope was injected. During the first 48 h of the metabolic study, the subjects were given equal portions of a fat-free energy drink (240 g of Genisoy powder and 850 g strawberry sorbet, 58 g sugar per 1,000 ml) at 10 AM, 1 PM, 4 PM, 7 PM, and 10 PM, to minimize the intermittent influx of intestinal chylomicrons, which might interfere with the kinetics of TRL apoB (20, 21). The feeding protocol began 2 h after the isotope was administered.

Isolation of lipoprotein fractions

The TRL (d < 1.019 g/ml) and total LDL (d = 1.019–1.063 g/ml) fractions were isolated from fresh plasma by sequential density ultracentrifugation. Isolated as d < 1.019 g/ml, the TRL fraction was a heterogeneous mixture of chylomicrons, VLDLs, and IDLs, even though the subjects consumed a fat-free energy drink. This fractionation was part of the original study protocol and was selected primarily to compare the metabolism of apoB-100 in lipoproteins with d < 1.019 g/ml with the metabolism of apoB-100 in total LDL (see Discussion) (16). In the original protocol, 3–4 ml of plasma from each timepoint of the metabolic study was

adjusted to $d = 1.019$ g/ml with potassium bromide (KBr). After ultracentrifugation, the top 0.5–0.75 ml was recovered as TRL; the middle layer (1.0–1.25 ml) was aspirated and discarded; and the bottom ($d > 1.019$ g/ml) layer was transferred to a fresh tube, and the density of the solution was increased to $d = 1.063$ g/ml in order to isolate LDLs. The top 0.5–0.75 ml layer recovered as LDLs was transferred to a fresh tube, overlaid with KBr $d = 1.063$ g/ml, and recentrifuged to guard against potential contamination of the recovered LDLs by TRL and HDL particles. The recovered TRL and LDL aliquots were frozen at −80°C until analysis, without being dialyzed.

To separate the LDL subfractions for the present study, an aliquot of undialyzed total LDL was diluted 2:1 with Dulbecco's PBS (Gibco, Life Technologies, Grand Island, NY), thereby adjusting the solution density to $d = 1.044$ g/ml, and then centrifuged at 171,919.7 g for 41 h by using a Beckman 50.3 Ti rotor (Beckman, Brea, CA). The recovered top 30% of the LDL solution represented lbLDLs ($d = 1.019$–1.044 g/ml) and the recovered bottom portion represented sdLDLs ($d = 1.044$–1.063 g/ml). The isolated LDL subfractions were frozen immediately at −80°C and stored for up to 18 months until analysis.

Plasma lipid and apoB determinations

Lipid and apoB levels were measured in five plasma samples collected during the continuous feeding period (mean of 2, 4, 6, 8, and 10 h). Plasma concentrations of TC, TGs, total LDL cholesterol, sdLDL cholesterol, and HDL cholesterol were assessed by automated online assays. TRL cholesterol concentration was calculated as the difference between TC and the sum of total LDL and HDL cholesterol; and lbLDL cholesterol was calculated as the difference between total LDL cholesterol and sdLDL cholesterol. To determine the concentration of apoB-100 in TRLs, lbLDLs, and sdLDLs, the concentration of plasma total apoB, TRL apoB, and apoB in each LDL subfraction recovered after ultracentrifugation was measured by an immunoturbidometric method using standardized reagents from Kamiya Diagnostics (Seattle, WA). The relative proportion of apoB recovered in lbLDLs and sdLDLs was multiplied by the concentration of apoB in total LDL, which was calculated by subtracting the concentration of TRL apoB from plasma total apoB. No correction was made for apoB-48, determined in our previous studies to represent <5% of the total apoB concentration in the $d < 1.019$ g/ml fraction when study subjects with combined hyperlipidemia were in the fed state (14). For kinetic analysis (see below), apolipoprotein plasma concentrations were converted to pool size (PS) by using the following formula:

$$\text{PS(mg)} = [\text{apolipoprotein concentration(mg/l)} \times \text{plasma volume(l)}].$$

Plasma volume was estimated as 4.5% of body weight (in kg).

ApoB-100 separation, isotopic enrichment, and kinetic analysis

The protocols for the separation of apoB-100, the determination of isotopic enrichment, and the kinetic analysis were performed as previously described (14). Plasma-free amino acids were isolated from the TCA extract of whole plasma by cation exchange chromatography, using AG50W-X8 100–200 mesh, H⁺ resin (Bio-Rad Laboratories, Hercules, CA). GC/MS selected ion monitoring at m/z 349 (derivatized leucine − HF)⁻ and m/z 352 (derivatized D$_3$-leucine − HF)⁻ was used to determine the areas under the chromatographic peaks for each ion. Percent deuterated leucine enrichment (D$_3$-leucine/[D$_3$-leucine + leucine]) for each sample was calculated from the area under the curve and corrected for the isotopic enrichment of the D$_3$-leucine tracer

(22). The isotopic enrichment of the tracer used in this study was 99.94%, as analyzed by GC/MS.

The kinetic parameters of apoB-100 were assessed by using a compartment model and the SAAM II program (The Epsilon Group, Charlottesville, VA). As presented in **Fig. 1**, the model consisted of a four-compartment leucine subsystem (compartments 1–4), which describes the plasma kinetics of the D$_3$-leucine tracer. Tracer was injected via the plasma compartment, compartment 2; samples were also collected from plasma for the measurement of leucine enrichment. Initially, the subsystem was fit to the plasma leucine enrichment data to estimate the fractional rate constants between compartments 1–4 together with the irreversible loss rate constant from compartment 2 (see supplemental Table S1 for model parameters). These rate constants were fixed, while the apoB section of the model was fit to the TRL, lbLDL, and sdLDL apoB enrichment data. A fraction of leucine from compartment 2 entered an intrahepatic pool, compartment 5, which accounted for the time required for the synthesis, assembly, and secretion of apoB-100 into plasma. A second delay compartment (compartment 10) represented the remodeling of apoB-containing particles that occurs in the hepatic extravascular space. Compartment 10 was required in order to fit the lbLDL and sdLDL apoB-100 enrichment data. The presence of a delay between TRL and LDL apoB-100 has been reported previously, with studies suggesting that TRLs may leave the plasma and reappear later in LDLs (23, 24). The model provides for the direct secretion of apoB into the TRL, lbLDL, and sdLDL fractions, as well as the extrahepatic delipidation of TRL to LDL. Four intravascular compartments (compartments 6–9) described the kinetics of apoB-100 in the TRL plasma fraction and allowed for a delipidation cascade (compartments 6–8) and a slowly turning over TRL pool (compartment 9) (25). ApoB in compartment 9 could potentially be converted to LDL, although we could not resolve this pathway with any degree of precision during model fitting. TRL apoB-100 can be converted to lbLDL or sdLDL or removed directly from plasma. The metabolism of the LDL subfractions is described by two distinct compartments. The compartment representing lbLDL was derived from direct secretion from the hepatocytes and the conversion of TRL to lbLDL (compartment 11) and allows for the extravascular remodeling of these particles (compartment 12). The compartment representing sdLDL (compartment 13) was derived from three sources: the conversion of lbLDL to sdLDL, the conversion of TRL to sdLDL, and de novo hepatic synthesis. ApoB in compartment 13 could potentially exchange with an extravascular compartment; however, this could not be resolved during model fitting, in part because of the relatively short duration of the kinetic study. Because an extravascular compartment was not included in the final model, the fractional catabolic rate (FCR) estimated by using this model might be an overestimate of the true FCR of sdLDL particles.

The FCRs of TRL apoB-100, lbLDL apoB-100, and sdLDL apoB-100 were derived from the model parameters giving the best fit. Production rate (PR) was computed by using the following formula:

$$\text{PR}(\text{mg/kg} \cdot \text{day}^{-1}) = \text{FCR}(\text{pools/day})$$
$$\times \text{apolipoprotein concentration}(\text{mg/l})$$
$$\times \text{plasma volume}(\text{l})/\text{body weight}(\text{kg})$$

LDL subfraction proteomic analysis

Proteomic analysis of lbLDL and sdLDL particles was assessed by in-solution tryptic digestion and LC/MS using an Agilent 6550 quadrupole TOF mass spectrometer with a Chip Nano source (Agilent Technologies, Santa Clara, CA). Briefly, apoB-depleted aliquots of lbLDLs and sdLDLs were reduced in 20 mM Tris[2-carboxyethyl]phosphine for 5 min at 95°C, alkylated in 10 mM
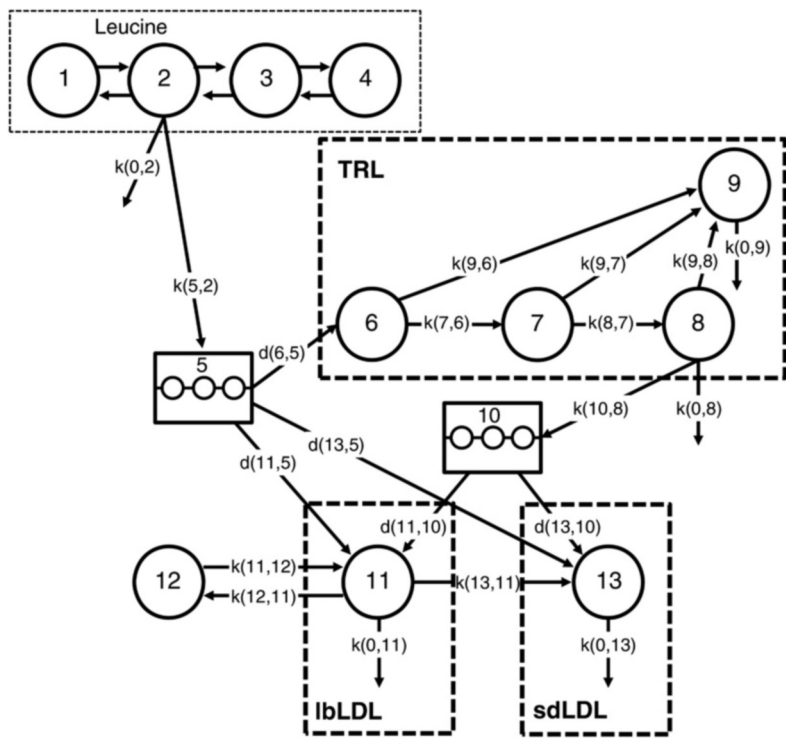
Fig. 1. Compartment model for the metabolism of leucine and apoB-100 in TRL, lbLDL, and sdLDL. Compartments 1–4 represent the kinetics of plasma leucine after the injection of D_3-leucine, which is injected into plasma, compartment 2. Plasma leucine exchanges between extravascular compartments (compartments 1, 3, and 4). A fraction of the leucine pool is directed to an intrahepatic delay compartment, compartment 5, which accounts for the time required for the synthesis, assembly, and secretion of apoB-100 into plasma. A second delay compartment (compartment 10) represents the lipolytic remodeling of apoB-containing particles that occurs in the hepatic extravascular space. Compartments 6–9 describe the kinetics of TRL apoB-100 in plasma and allow for a delipidation cascade (compartments 6–8) and a slowly turning over TRL pool (compartment 9). Compartment 11 representing lbLDL apoB-100 is derived from direct secretion of apoB-100 from the hepatocytes and the conversion of TRL particles to lbLDL particles and allows for the extravascular remodeling of these particles (compartment 12). Compartment 13, representing sdLDL, is derived from three sources: the conversion of lbLDL to sdLDL, the conversion of TRL to sdLDL, and de novo hepatic synthesis. The rectangle with thin dotted lines indicates the leucine model, consisting of vascular and extravascular compartments; the rectangles with thick dashed lines denote the plasma compartments of TRL, lbLDL, and sdLDL apoB-100.

iodoacetamide for 20 min at room temperature, and then incubated in a 6.6 ng/μl solution of sequencing-grade trypsin (Promega, Madison, WI) at 37°C for 5 h. The digested peptides were desalted with a C18 ZipTip pipette tip and eluted with 1% formic acid before analysis.

The tryptic peptides were separated chromatographically by using a Polaris HR chip (Agilent Technologies) consisting of a 360 nl enrichment column and a 0.075 × 150 mm analytical column, each packed with Polaris C18-A stationary phase with 2 μm particle size. The mobile phase was 5% acetonitrile and 0.1% formic acid (buffer A) (Honeywell/Burdick and Jackson, Muskegon, MI) and 95% acetonitrile and 0.1% formic acid (buffer B) (Honeywell/Burdick and Jackson). For optimal data acquisition, equal amounts of the peptides from each sample were injected onto the column. Peptides were eluted at a flow rate of 0.4 μl/min with sequential linear gradients of 2%→5% buffer B over 0.5 min, 5%→30% buffer B over 9.5 min, and 30%→5% buffer B over 3 min, followed by 5.1 min with 90% buffer B and 12.9 min of equilibration with 2% buffer B. Data-dependent MS/MS peptide spectra were collected, four mass spectrometry scans/s, with up to six MS/MS spectra from each scan.

To establish protein identification, the MS/MS data were analyzed with Spectrum Mill (Agilent Technologies, Rev B.04.00.127) and searched against the human sequences in the Uniprot/Swissprot database (downloaded 05/2013). Peptide-to-spectrum matching criteria included a precursor ion mass tolerance ⩽15 ppm and a MS/MS fragment mass deviation ⩽30 ppm. Tryptic peptides having up to two missed cleavage sites, fixed carbamidomethylation of the cysteine residues, variable oxidation of the methionine residues, and variable pyroglutamic acid modification were allowed in the search. The database was then restricted to the proteins observed in the first Spectrum Mill search, and a second search of the fragmentation data was performed allowing for nonspecific cleavage of the proteins. Peptides were identified with a false discovery rate ⩽1%. The relative abundance of each protein was inferred from the summed peptide ion current.

Proteomic analysis could not be achieved in one subject due to technical difficulties; therefore, the data represent the analysis of five subjects.

Statistical analysis

The SAS System for Windows (release 9.2; SAS Institute, Cary, NC) was used for statistical analysis. A logarithmic transformation was applied to the data not normally distributed before formal analysis. Significant differences in the means between placebo and treatment phases and between lbLDL and sdLDL kinetic parameters were assessed by paired t-test analysis. The percent change relative to placebo was calculated on an individual basis and summarized descriptively. All data in the text, tables, and figures are presented in the original scale of measurement as means ± SEM. $P < 0.05$ was considered significant.

RESULTS

As reported previously, inhibition of HMG-CoA reductase with rosuvastatin 40 mg/day markedly lowered non-fasting plasma concentrations of TC (-37%, $P < 0.0001$), TGs (-32%, $P = 0.06$), LDL cholesterol (-52%, $P < 0.001$), and total apoB (-42%, $P < 0.0001$), as compared with placebo (**Table 1**) (16). Rosuvastatin also significantly ($P < 0.01$) reduced the concentrations of apoB and cholesterol within lbLDLs (apoB, -39%; cholesterol, -48%) and sdLDLs (apoB, -42%; cholesterol, -54%) (**Fig. 2**). In both the placebo and the rosuvastatin phases, the absolute concentration of apoB in sdLDLs was at least 2.5 times greater than the concentration of apoB in lbLDLs. The converse was true for absolute cholesterol concentrations, with twice as much cholesterol being present in lbLDLs than in sdLDLs. Relative to placebo, rosuvastatin decreased the cholesterol content per particle from 940 ±

TABLE 1. Effects of rosuvastatin on nonfasting plasma lipid and apolipoprotein concentrations

Parameter	Placebo	Rosuvastatin 40 mg/day	Change, %
Cholesterol, mmol/l			
Total	5.83 ± 0.26	3.69 ± 0.23[a]	−37 ± 2
TRL	0.78 ± 0.12	0.57 ± 0.04	−19 ± 15
LDL	3.80 ± 0.24	1.86 ± 0.27[b]	−52 ± 5
sdLDL	1.26 ± 0.22	0.56 ± 0.09[c]	−54 ± 4
HDL	1.29 ± 0.15	1.27 ± 0.13	0.2 ± 5
TGs, mmol/l	2.11 ± 0.47	1.29 ± 0.32[d]	−32 ± 10
ApoB, g/l	0.99 ± 0.06	0.58 ± 0.06[a]	−42 ± 3

Data are presented as mean ± SEM, n = 6. To convert total, LDL, HDL, and TRL cholesterol in mmol/l to mg/dl, multiply by 38.67; TGs in mmol/l to mg/dl, multiply by 88.57. The percent change relative to placebo is the mean of the percent change calculated on an individual basis. Significance for comparison of absolute values with placebo phase was determined by using a paired t-test, with TGs being log-transformed before statistical analysis.
[a] $P < 0.0001$, for comparison with placebo phase.
[b] $P = 0.0002$.
[c] $P = 0.003$.
[d] $P = 0.06$.

128 mol to 719 ± 66 mol (−19%, $P = 0.06$) in sdLDLs and from 5,536 ± 518 mol to 4,552 ± 405 mol (−14%, $P = 0.18$) in lbLDLs (supplemental Table S2); however, the cholesterol:apoB molar ratio in sdLDLs, relative to lbLDLs, did not change significantly ($P = 0.55$). The concentration of sdLDL cholesterol was, on average, approximately 32% of total LDL cholesterol during both phases.

Figure 3 illustrates the isotopic enrichment of apoB-100 in lbLDLs and sdLDLs over the course of the metabolic study (0–69 h). The appearance of deuterated leucine in sdLDL apoB-100 occurred at a slower rate compared with lbLDL apoB-100. In addition, the maximum isotopic enrichment in sdLDL apoB-100 was markedly lower than that in lbLDL apoB-100 in both the placebo (Fig. 3A) and the rosuvastatin (Fig. 3B) phases. The enrichment of sdLDL apoB-100 at its maximum was approximately equal to that of lbLDL, indicating that apoB-100 in lbLDL was a partial precursor of sdLDL apoB-100. The crossover of the two enrichment curves occurred earlier in the rosuvastatin phase compared with the placebo phase (placebo: ∼35–40 h; rosuvastatin: ∼20 h), in part a consequence of the relatively smaller apoB-100 mass associated with the extravascular compartment (compartment 12 in Fig. 1) and the more rapid turnover of the lbLDL and sdLDL particles relative to the placebo phase. The compartment model giving the best

fit to the data (Fig. 1) supported this precursor-product relationship between the two LDL subfractions. In addition, a clear precursor-product relationship between TRL apoB-100 and lbLDL apoB-100 and between TRL apoB-100 and sdLDL apoB-100 was observed during both phases (supplemental Fig. S1).

As shown in **Table 2**, the rosuvastatin-induced decrease in apoB-100 PS in all fractions was attributable to significant ($P \leq 0.01$) increases in the catabolism of apoB-100. Relative to placebo, rosuvastatin increased the FCR of apoB-100 in TRL, lbLDL, and sdLDL by 45 ± 16%, 131 ± 66%, and 97 ± 32%, respectively, with no significant effects on apoB-100 PR. During both the placebo and rosuvastatin phases, sdLDL apoB-100 was catabolized at a slower fractional rate (placebo, 0.36 ± 0.06 pools/day; rosuvastatin, 0.69 ± 0.14 pools/day) than lbLDL apoB-100 (placebo, 0.63 ± 0.10 pools/day; rosuvastatin, 1.23 ± 0.24 pools/day; both $P \leq 0.01$). The sdLDL apoB-100 PR was higher than the lbLDL apoB-100 PR (placebo, 10.39 ± 1.29 vs. 6.31 ± 0.64 mg/kg·day^{-1}, $P \leq 0.01$; rosuvastatin, 11.03 ± 1.21 vs. 7.35 ± 0.95 mg/kg·day^{-1}, $P \leq 0.001$). During the placebo phase, 25% of TRL apoB-100 was cleared directly from the circulation, presumably by the liver; 37% was converted from TRL to lbLDL; 38% went directly from TRL to sdLDL apoB; and all lbLDL apoB-100 was converted to sdLDL. Statin therapy did not alter these distributions significantly.

Direct production of apoB-100 into the LDL subfractions was also not altered significantly by rosuvastatin therapy (Table 2). During the placebo phase, most of the lbLDL apoB-100 was derived from TRL apoB-100 (73.6%), with the remainder (26.4%) being secreted de novo by the liver. Most of the sdLDL apoB-100 (61.4%) was derived from lbLDL apoB-100, with 35.9% from TRL apoB-100 and 2.7% from de novo hepatic synthesis. Similarly, during the rosuvastatin phase, 71.2% of the lbLDL apoB-100 was derived from TRL apoB-100 and 28.8% via de novo hepatic production. Most of the sdLDL apoB-100 was derived via lipolysis of larger apoB-100-containing particles (66.2% from TRL apoB-100; 30.4% from lbLDL apoB-100), and only 3.3% was produced de novo.

Proteomic analysis of the lbLDL and sdLDL subfractions indicated the presence of the following apolipoproteins, in addition to apoB, in the density range of both subfractions: apoA-I, apoA-II, apoA-IV, apoC-I, apoC-II, apoC-III, apoC-IV, apoD, apoE, apoF, and apoM (**Table 3**). The total protein
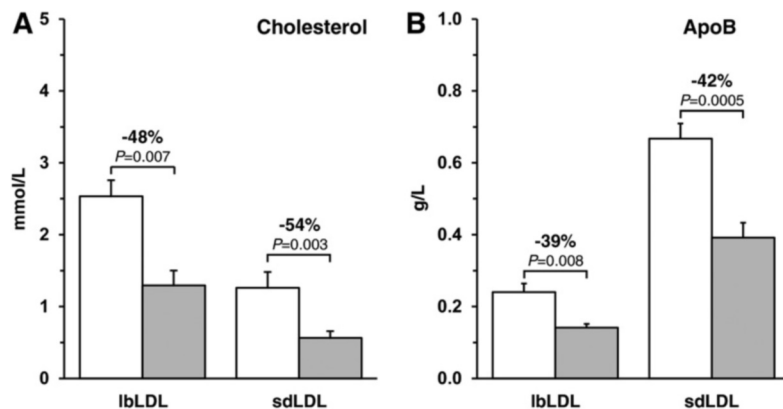

Fig. 2. Cholesterol (A) and apoB-100 (B) concentrations in lbLDL and sdLDL during the placebo and rosuvastatin 40 mg/day phases. Data are expressed as mean ± SEM (n = 6). White bar, placebo phase; shaded bar, rosuvastatin phase.
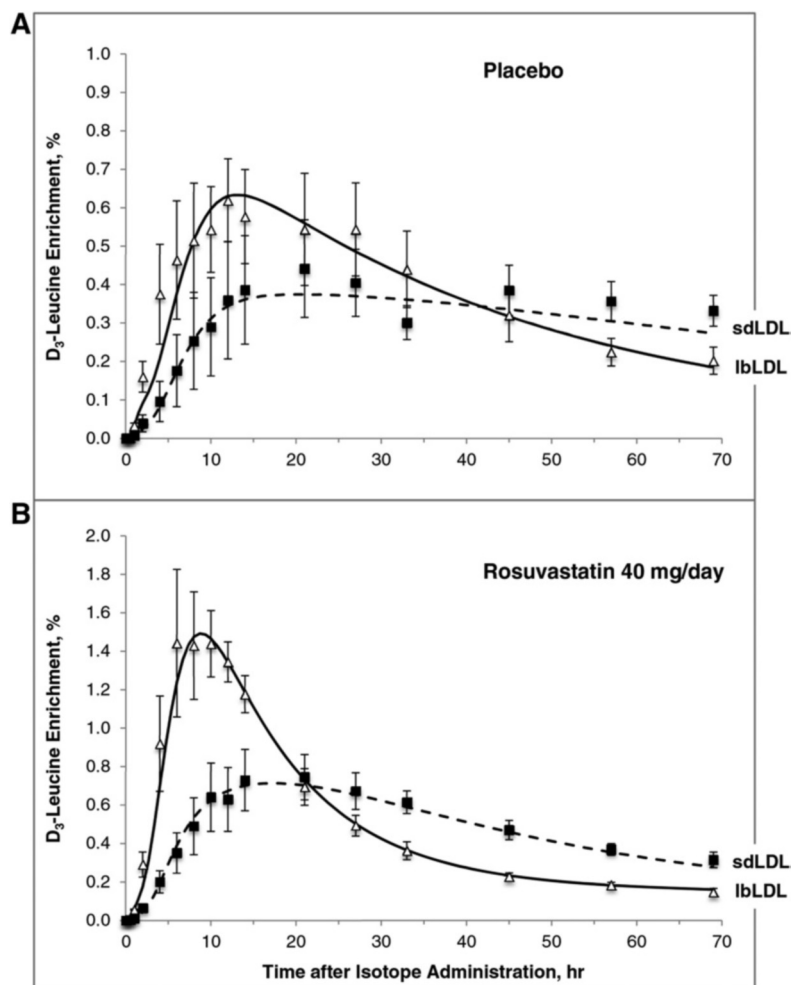
Fig. 3. D_3-leucine percent enrichment of apoB-100 in lbLDL and sdLDL during the placebo (A) and rosuvastatin 40 mg/day (B) phases. The graphs depict the fit of the model to the enrichment data derived from the GC/MS analysis. The points represent enrichment (mean ± SEM, n = 6); lines denote the model-predicted values. Open triangles and solid line indicate apoB-100 in lbLDL; filled squares and dashed line indicate apoB-100 in sdLDL.

spectral intensity, log base 2, of each apolipoprotein, as calculated by Agilent Spectrum Mill, was greater in sdLDLs than in lbLDLs, with the exception of apoC-II and apoE, during the placebo phase. Significant differences ($P < 0.05$) between the two subfractions were noted for apoA-I and apoA-IV during the placebo phase and for apoA-IV, apoC-III, and apoM during rosuvastatin treatment. ApoA-IV was not associated with lbLDLs in either the placebo or the rosuvastatin phase. Rosuvastatin lowered the abundances of all detected apolipoproteins in lbLDLs except apoA-I, with notable decreases occurring in apoC-III ($-6.9 \pm 2.3\%$, $P = 0.04$), apoM ($-80.2 \pm 19.8\%$, $P = 0.02$), apoA-II ($-58.1 \pm 25.7\%$, $P = 0.08$), and apoD ($-1.3 \pm 0.5\%$, $P = 0.07$). In sdLDLs, only the abundance of apoA-IV was reduced significantly ($-3.1 \pm 1.0\%$, $P = 0.04$). Other proteins found to be present in sdLDLs in some subjects were carbamoyl-phosphate synthase, clusterin (apoJ), complement C3, hemoglobin subunits α and delta, histone H4, IgG kappa chain C region, serum amyloid A, and serum amyloid A4. The proteome of lbLDL particles included histone H3 and serum amyloid A4. Because the proteomic analysis was performed on apoB-depleted aliquots of the ultracentrifugally isolated LDL subfractions, to enhance the detection of low-abundance proteins, differences in the posttranslational modification of apoB-100 in sdLDLs and lbLDLs, like oxidation or carbamidomethylation, could not be detected.

DISCUSSION

Epidemiological studies including the Framingham Offspring Study, MESA, and ARIC have demonstrated that sdLDL cholesterol is a significantly better predictor of CVD than total LDL cholesterol (4–6). The assay used in these studies measured the cholesterol content of LDL particles in the density range of 1.044–1.063 g/ml (3). We defined sdLDL in an identical fashion and measured the metabolism of apoB-100 and the protein composition of this LDL subfraction relative to lbLDL in the density range of 1.019–1.044 g/ml. We found that sdLDL apoB-100 had a significantly longer plasma residence time (3.10 days) than lbLDL apoB-100 (1.95 days) in subjects with combined hyperlipidemia and that rosuvastatin significantly decreased these residence times by more than 40%, without altering production.

Previous studies have examined the metabolism of apoB in large and small LDLs by using stable isotopes (see supplemental Table S3) (26–28). Campos et al. (26) reported a plasma residence time of apoB-100 within dense LDLs ($d = 1.036–1.063$ g/ml) of 2.44 days and in light LDLs ($d = 1.019–1.036$ g/ml) of 1.69 days in eight postmenopausal women in the fed state. Aguilar-Salinas et al. (27) studied five subjects with combined hyperlipidemia in the fasting state while on placebo and then later on pravastatin

TABLE 2. Effects of rosuvastatin 40 mg/day on the PS, FCR, and PR of apoB-100 in TRL and LDL subfractions

	Placebo	Rosuvastatin	Change, %
TRL apoB-100			
Pool size, mg	283 ± 64	179 ± 41[a]	−32 ± 6
FCR, pools/day	3.37 ± 0.53	4.75 ± 0.71[b]	45 ± 16
PR, mg/kg·day^{-1}	12.64 ± 2.14	12.34 ± 2.45	−0.1 ± 9
RT, h	7.79 ± 0.90	5.65 ± 0.87	−26 ± 9
lbLDL apoB-100			
Pool size, mg	812 ± 68	493 ± 60[a]	−39 ± 5
FCR, pools/day	0.63 ± 0.10	1.23 ± 0.24[b]	131 ± 66
PR, mg/kg·day^{-1}	6.31 ± 0.64	7.35 ± 0.95	23 ± 20
RT, day	1.95 ± 0.48	0.95 ± 0.15	−42 ± 11
sdLDL apoB-100			
Pool size, mg	2321 ± 264	1363 ± 198[a]	−41 ± 4
FCR, pools/day	0.36 ± 0.06[c]	0.69 ± 0.14[b,c]	97 ± 32
PR, mg/kg·day^{-1}	10.39 ± 1.29[e]	11.03 ± 1.21[d]	12 ± 16
RT, day	3.10 ± 0.36[e]	1.75 ± 0.31[b,c]	−42 ± 10
% conversion			
TRL to lbLDL	37.27 ± 5.55	41.88 ± 8.82	10 ± 15
TRL to sdLDL	37.65 ± 10.36	36.89 ± 11.30	5 ± 28
TRL cleared directly by liver	25.08 ± 9.22	21.24 ± 11.95	−19 ± 31
lbLDL to sdLDL	100	100	0
Direct apoB-100 production			
TRL, de novo hepatic synthesis			
mg/kg·day^{-1}	12.64 ± 2.14	12.34 ± 2.45	−0.1 ± 9
% of total TRL apoB-100	100	100	0
% of total apoB-100 secreted	84.81 ± 6.89	81.87 ± 8.97	−5 ± 5
lbLDL, de novo hepatic synthesis			
mg/kg·day^{-1}	1.36 ± 0.36	2.02 ± 0.98	32 ± 27
% of total lbLDL apoB-100	26.43 ± 11.82	28.77 ± 13.09	19 ± 32
% of total apoB-100 secreted	12.99 ± 6.50	15.67 ± 8.39	20 ± 14
lbLDL, from TRL			
mg/kg·day^{-1}	4.95 ± 0.92	5.33 ± 1.36	6 ± 14
% of total lbLDL apoB-100	73.57 ± 11.82	71.23 ± 13.09	−9 ± 9
sdLDL, de novo hepatic synthesis			
mg/kg·day^{-1}	0.28 ± 0.05	0.36 ± 0.11	66 ± 57
% of total sdLDL apoB-100	2.70 ± 0.37	3.35 ± 0.88	37 ± 40
% of total apoB-100 secreted	2.20 ± 0.49	2.46 ± 0.67	56 ± 55
sdLDL, from TRL			
mg/kg·day^{-1}	3.80 ± 0.71	3.31 ± 0.45	−4 ± 18
% of total sdLDL apoB-100	35.90 ± 2.79	30.43 ± 3.15	−13 ± 13
sdLDL, from lbLDL			
mg/kg·day^{-1}	6.31 ± 0.64	7.35 ± 0.95	23 ± 20
% of total sdLDL apoB-100	61.40 ± 3.11	66.22 ± 2.65	9 ± 7

RT, plasma residence time. Data are presented as mean ± SEM, n = 6. The percent change relative to placebo is the mean of the percent change calculated on an individual basis. Significance for comparison of absolute values with placebo phase and for comparison of sdLDL with lbLDL was determined by using a paired *t*-test.

[a]$P \leqslant 0.01$, for comparison with placebo phase.

[b]$P < 0.05$.

[c]$P \leqslant 0.01$.

[d]$P \leqslant 0.001$, for comparison with lbLDL.

[e]$P < 0.05$.

therapy (20 mg/day). They observed a mean apoB plasma residence time on placebo and statin of 5.11 and 2.82 days for dense LDLs (d = 1.035–1.063 g/ml) and 1.31 and 0.80 days for light LDLs (d = 1.019–1.035 g/ml), respectively (27). Zheng et al. (28) fractionated LDLs into light (d = 1.025–1.032 g/ml), medium (d = 1.032–1.038 g/ml), and dense (d = 1.038–1.050 g/ml) subclasses and examined apoB metabolism in 12 normolipidemic and 9 hypertriglyceridemic subjects in the fed state. In their study, plasma was separated by immunoaffinity chromatography, before ultracentrifugation, into four fractions based on apoC-III and apoE content. In all three LDL density ranges, the major LDL particle, making up >90% of total LDL, contained neither apoC-III nor apoE, and the observed apoB residence times in normal subjects were approximately 0.3 days in light LDLs, 0.67 days in medium LDLs, and 0.85 days in dense LDLs. Notably, this study omitted the densest LDL fraction (d = 1.050–1.063 g/ml). Discrepancies among the reported plasma residence times, in our opinion, relate to the selection of study subjects; the study design, including modeling of tracer data; and the feeding status of the subjects during the metabolic study. Hyperlipidemic subjects often have delayed LDL apoB-100 catabolism (see supplemental Table S3). We have documented also that feeding results in more direct TRL apoB-100 catabolism and less conversion of TRL apoB-100 to LDL apoB-100, as well as delayed LDL apoB-100 catabolism, compared with the fasting state (29). Despite the differences, our findings are consistent with these previous studies and support the concept that apoB in sdLDLs is catabolized more slowly than apoB in lbLDLs.

Our data indicate that approximately 80% of lbLDL apoB-100 is derived from TRL apoB-100, with the remainder

Proteins	Placebo (total protein spectral intensity, log base 2)			Rosuvastatin (total protein spectral intensity, log base 2)			Rosuvastatin vs. placebo,[a] change, % (P)	
	lbLDL	sdLDL	P^b	lbLDL	sdLDL	P^b	lbLDL	sdLDL
ApoA-I	19.9 ± 0.9	22.8 ± 0.5	0.03	20.4 ± 0.9	22.9 ± 0.5	0.09	2.6% (0.64)	0.8% (0.74)
ApoA-II	19.0 ± 0.5	19.3 ± 0.7	0.72	7.9 ± 4.8	19.2 ± 0.3	0.08	−58.1% (0.08)	−0.2% (0.88)
ApoA-IV	0	14.7 ± 3.7	0.02	0	14.1 ± 3.5	0.02	0	−3.1% (0.04)
ApoC-I	9.1 ± 5.6	19.8 ± 1.0	0.16	7. ± 4.9	19.8 ± 0.6	0.07	−2.1% (0.87)	0.7% (0.97)
ApoC-II	22.0 ± 0.1	20.3 ± 0.9	0.11	20.2 ± 0.8	20.4 ± 0.4	0.78	−8.2% (0.11)	1.3% (0.94)
ApoC-III	23.4 ± 0.3	23.4 ± 0.4	0.93	21.8 ± 0.5	23.5 ± 0.2	0.02	−6.9% (0.04)	0.4% (0.92)
ApoC-IV	10.1 ± 4.1	13.3 ± 3.3	0.64	3.3 ± 3.3	13.4 ± 3.4	0.07	−40.6% (0.17)	0.1% (0.95)
ApoD	12.8 ± 5.2	20.7 ± 0.4	0.21	12.5 ± 5.1	20.5 ± 0.4	0.19	−1.3% (0.07)	−1.3% (0.46)
ApoE	23.5 ± 1.1	22.7 ± 0.4	0.53	22.3 ± 1.8	22.5 ± 0.4	0.92	−5.6% (0.30)	−0.6% (0.81)
ApoF	11.7 ± 4.8	21.1 ± 0.6	0.13	11.6 ± 4.7	20.9 ± 0.2	0.12	−0.6% (0.79)	−0.7% (0.70)
ApoM	18.5 ± 0.3	19.7 ± 0.8	0.31	3.8 ± 3.8	18.8 ± 0.4	0.01	−80.2% (0.02)	−3.6% (0.43)

Data are presented as the total protein spectral intensity, log base 2, of the individual proteins, as calculated by Agilent Spectrum Mill (Agilent Technologies), mean ± SEM, n = 5.

[a]Percent change relative to placebo was calculated on an individual basis and summarized descriptively by LDL subfraction. Significance for comparison of rosuvastatin phase absolute values with placebo phase absolute values was determined by using a paired t-test.

[b]Significance for comparison of sdLDL with lbLDL was determined by using a paired t-test.

being produced directly. They also show that approximately 60% of sdLDL apoB-100 is derived from lbLDL apoB-100, with most of the remainder coming directly from TRL apoB-100. There does appear to be a small percentage of sdLDL apoB-100 derived from direct liver production. These percentages are not greatly altered with rosuvastatin therapy for either lbLDL apoB-100 or sdLDL apoB-100. In this study, we did not subfractionate the TRL fraction, and, therefore, we were unable to ascertain which portion of the TRL fraction may have been the precursor of, or contributed more to, the sdLDL fraction, compared with the lbLDL fraction or how rosuvastatin may have modified the delipidation cascade more specifically. Aguilar-Salinas et al. (27) concluded that "a clear precursor-product relationship" was observed between the VLDL, IDL, light LDL and dense LDL fractions. In contrast, Zheng et al. (28) found that 83% of sdLDL apoB-100 was derived directly from IDLs, with only 8% being derived from lbLDLs. Packard and colleagues (30–32) did not examine the metabolism of LDL subfractions directly; however, they did propose that, in subjects with moderate hypertriglyceridemia, there is likely to be increased conversion of large VLDL apoB-100 directly to sdLDL. It should be noted that the separation of LDL subfractions probably results in the isolation of heterogeneous populations of particles that have different metabolic and, hence, kinetic properties.

It was important to examine differences in the proteome of lbLDLs and sdLDLs on both placebo and rosuvastatin, which potentially might explain the difference in the catabolic rate of apoB in lbLDLs and sdLDLs. Earlier studies of LDL composition have reported that apolipoproteins A-I, A-II, C-I, C-II, C-III, C-IV, D, E, and F, in addition to apoB, as well as clusterin, complement C3, C4a, and C4b, and paraoxonase 1 are associated with LDL particles (11, 17–19). Davidsson et al. (33) examined the protein content of LDL subfractions of d = 1.030–1.040 and 1.040–1.063 g/ml and observed a higher apoC-III content and a lower content of apoA-I, apoC-I, and apoE in sdLDLs versus lbLDLs. Moreover, in subjects with metabolic syndrome and diabetes, there were not only excess sdLDLs, but also greater apoC-III enrichment of sdLDLs than in normal subjects (33).

We also found that the proteomes of the lbLDL and sdLDL subfractions separated by ultracentrifugation were different. Apolipoproteins A-I, A-II, C-I, C-II, C-III, C-IV, D, E, F, and M were associated with both lbLDL and sdLDL density fractions, whereas apoA-IV was associated only with the sdLDL density fraction. On placebo, the sdLDL subfraction had significantly higher apoA-I content than did the lbLDL subfraction. Rosuvastatin treatment resulted in significant decreases in the apoA-IV content of sdLDLs and in the apoC-III and apoM content of lbLDLs as compared with placebo. The effects on apoM were very striking. Data derived from proteomic analyses based on lipoprotein particles isolated by ultracentrifugation should be viewed with caution. Weakly associated proteins are well known to redistribute from one lipoprotein fraction to another during ultracentrifugation, due to high shear forces and the ionic strength of preparative solutions. Although the procedure used to isolate the total LDL fraction in the larger metabolic study included reultracentrifugation in order to guard against potential contamination by TRL and HDL particles (see Materials and Methods), a more specific isolation procedure, namely, immunoprecipitation with a monoclonal antibody against human apoB, with or without ultracentrifugation, would have had the advantage of determining whether the LDL subfractions do indeed contain protein components that are normally thought to be associated with HDLs, such as apoA-I.

Further studies are required to understand fully the function of many of the identified apolipoproteins in humans. It is known, however, that apoC-III inhibits lipoprotein lipase activity and the hepatic uptake of TRL; therefore, its presence may prolong the residence time of apoB-100-containing lipoproteins (34, 35). The reduction in apoC-III associated with lbLDL during the rosuvastatin phase may, as a result, contribute to the significant increase in apoB clearance. Alternatively, and in our opinion more likely, the enhanced LDL apoB-100 clearance induced by statins relates to the inhibition of cellular cholesterol synthesis and up-regulation of LDL receptor activity. In previous studies, we documented significant differences in lipid composition between sdLDLs and lbLDLs, indicating

that major apoB-100 conformational changes on the surface of sdLDLs, as compared with lbLDLs, were required to accommodate the smaller amount of lipid (35). At that time, we speculated that these changes would likely affect the binding of sdLDL to its receptor and its plasma residence time (36), a concept supported by competitive binding assays in human skin fibroblasts with LDL particles of different size (37). Our current data also support this hypothesis.

It is possible that the increased atherogenicity of sdLDLs is not only due to lipolysis and the subsequent alteration in particle size. Other factors may, at least in part, be responsible, such as the binding of apoB-containing lipoproteins to proteoglycans in the extracellular matrix of the arterial wall, which, in turn, would increase the time the particle spends trapped in the subendothelial space of the artery wall and stimulate uptake by macrophages. Anber et al. (38, 39) have demonstrated, using LDL isolated from dyslipidemic subjects with a lipid profile comparable to our study subjects, that the formation of arterial wall proteoglycan/LDL complexes was positively associated with the percentage of sdLDLs ($d = 1.044–1.063$ g/ml) in total LDL and plasma TG levels and negatively associated with the percentage of lbLDLs ($d = 1.019–1.033$ g/ml) and plasma HDL cholesterol levels. Furthermore, proteoglycan/LDL complex formation was significantly higher in the subjects with elevated sdLDL levels. In the present study, the proteomic analysis was performed by using apoB-depleted aliquots of the isolated LDL subfractions, and the differences in the posttranslational modifications of apoB-100 in sdLDLs, compared with apoB-100 in lbLDLs, which may have characterized the conformational changes and pointed to the primary reason(s) that sdLDL is particularly atherogenic, were not analyzed. Regardless of the precise mechanism, a prolonged plasma residence time would extend the period of exposure that the arterial wall has to the particle and, thus, would enhance the atherogenic potential of sdLDL.

A novel aspect of the present study was that the kinetics of LDL apoB-100 was examined in LDL density subfractions that match with those used in epidemiological and clinical studies. Although the importance of our findings is potentially limited by the small number of study subjects and relatively short duration of each kinetic study, the dyslipidemic phenotype of the subjects, and the feeding protocol used in the study, our data do indicate *1*) that a significant percentage of TRL apoB-100 (25% in this study) is catabolized directly; *2*) that the remaining TRL apoB-100 is converted directly and equally to both lbLDLs and sdLDLs; and *3*) that all lbLDL apoB-100 is converted to sdLDL apoB-100. These findings provide an explanation for the elevated sdLDL concentrations observed in hypertriglyceridemic subjects, potentially due to the increased direct conversion of TRL apoB-100 to sdLDL apoB-100. Packard et al. (30–32) have postulated convincingly that the key abnormality leading to the generation of sdLDL is the development of mild to moderate hypertriglyceridemia, defined as a plasma TG concentration > 1.5 mmol/l. Under these metabolic conditions, large-size VLDL$_1$ accumulates due to overproduction and/or delayed clearance; when lipolyzed, VLDL$_1$ gives rise to a population of small

LDLs, which fail to bind well to the LDL receptor and, therefore, have a longer plasma residence and increased likelihood of undergoing remodeling. Through the action of cholesteryl ester transfer protein, cholesteryl ester is exchanged for TG, resulting in TG-enriched LDL, a good substrate for hepatic lipase and, in turn, sdLDL (31).

The benefit of statins for decreasing CVD risk is underscored by the observation that rosuvastatin not only enhanced TRL and LDL apoB-100 fractional catabolism, but also significantly enhanced the fractional catabolism of apoB-100 in both lbLDL and sdLDL. We found that the concentration of apoB in sdLDLs was more than twice as high as that in lbLDLs, whereas the converse was true for the cholesterol concentrations, with twice as much cholesterol being present in lbLDLs than in sdLDLs. Treatment with rosuvastatin decreased the total number of lbLDL and sdLDL particles as measured by apoB concentrations, as well as the cholesterol content per particle. It did not, however, change the cholesterol:apoB molar ratio in sdLDLs relative to lbLDLs.

In conclusion, sdLDL apoB-100 was catabolized more slowly than lbLDL apoB-100 in subjects with combined hyperlipidemia during both the placebo and rosuvastatin (40 mg/day) treatment periods. Rosuvastatin enhanced the clearance of apoB-100 in both sdLDLs and lbLDLs, with no effect on production or on the conversion rates of TRL to LDL subfractions. There were differences in apolipoprotein composition and abundance between sdLDLs and lbLDLs, which may account for some of the differences in the atherogenicity of the LDL particles. We believe, however, that the increased plasma residence time of sdLDL apoB-100 relative to lbLDL apoB-100 is due to a change in apoB-100 conformation on the surface of sdLDLs, inhibiting receptor-mediated catabolism. Other factors, such as a preferential affinity for proteoglycans in the arterial wall, may have an effect in the atherogenicity of the different LDL particles. However, in our view, the major reason for the increased atherogenicity of sdLDL is its longer residence time in plasma, leading to an increased likelihood of lipolysis, posttranslational modification, oxidation, and enhanced uptake into the arterial wall.

REFERENCES

1. Cholesterol Treatment Trialists' (CTT) Collaboration; J. Fulcher, R. O'Connell, M. Voysey, J. Embeson, L. Blackwell, B. Mihaylova, J. Simes, R. Collins, A. Kirby, H. Colhoun, et al. 2015. Efficacy and safety of LDL-lowering therapy among men and women: meta-analysis of individual data from 174,000 participants in 27 randomized trials. *Lancet.* **385:** 1397–1405.
2. Krauss, R. M. 2010. Lipoprotein subfractions and cardiovascular disease risk. *Curr. Opin. Lipidol.* **21:** 305–311.

3. Hirano, T., Y. Ito, S. Koba, M. Toyoda, A. Ikejiri, H. Saegusa, J. Yamazaki, and G. Yoshino. 2004. Clinical significance of small dense low-density lipoprotein cholesterol levels determined by the simple precipitation method. *Arterioscler. Thromb. Vasc. Biol.* **24:** 558–563.

4. Ai, M., S. Otokozawa, B. F. Asztalos, Y. Ito, K. Nakajima, C. C. White, L. A. Cupples, P. W. Wilson, and E. J. Schaefer. 2010. Small dense LDL cholesterol and coronary heart disease: results from the Framingham Offspring Study. *Clin. Chem.* **56:** 967–976.

5. Tsai, M. Y., B. T. Steffen, W. Guan, R. L. McClelland, R. Warnick, J. McConnell, D. M. Hoefner, and A. T. Remaley. 2014. New automated assay of small dense low-density lipoprotein cholesterol identifies risk of coronary heart disease: the Multi-Ethnic Study of Atherosclerosis. *Arterioscler. Thromb. Vasc. Biol.* **34:** 196–201.

6. Hoogeveen, R. C., J. W. Gaubatz, W. Sun, R. C. Dodge, J. R. Crosby, J. Jiang, D. Couper, S. S. Virani, S. Kathiresan, E. Boerwinkle, et al. 2014. Small dense low-density lipoprotein-cholesterol concentrations predict risk for coronary heart disease: the Atherosclerosis Risk In Communities (ARIC) study. *Arterioscler. Thromb. Vasc. Biol.* **34:** 1069–1077.

7. Hirayama, S., and T. Miida. 2012. Small dense LDL: an emerging risk factor for cardiovascular disease. *Clin. Chim. Acta.* **414:** 215–224.

8. Bañuls, C., L. Bellod, A. Jover, M. L. Martínez-Triguero, V. M. Victor, M. Rocha, and A. Hernández-Mijares. 2012. Comparablity of two different polyacrylamide gel electrophoresis methods for the classification of LDL pattern type. *Clin. Chim. Acta.* **413:** 251–257.

9. Otvos, J. D., E. J. Jeyarahah, D. W. Bennett, and R. M. Krauss. 1992. Development of a proton nuclear magnetic resonance spectroscopic method for determining plasma lipoprotein concentrations and subspecies distributions from a single, rapid measurement. *Clin. Chem.* **38:** 1632–1638.

10. Caufield, M. P., S. Li, G. Lee, P. J. Blanche, W. A. Salameh, W. H. Benner, R. E. Reitz, and R. M. Krauss. 2008. Direct determination of lipoprotein particle sizes and concentrations by ion mobility analysis. *Clin. Chem.* **54:** 1307–1316.

11. Diffenderfer, M. R., and E. J. Schaefer. 2014. The composition and metabolism of large and small LDL. *Curr. Opin. Lipidol.* **25:** 221–226.

12. Ai, M., S. Otokozawa, B. F. Asztalos, K. Nakajima, E. Stein, P. H. Jones, and E. J. Schaefer. 2008. Effects of maximal doses of atorvastatin versus rosuvastatin on small dense low-density lipoprotein cholesterol levels. *Am. J. Cardiol.* **101:** 315–318.

13. Stone, N. J., J. G. Robinson, A. H. Lichtenstein, C. N. Bairey Merz, C. B. Blum, R. H. Eckel, A. C. Goldberg, D. Gordon, D. Levy, D. M. Lloyd-Jones, et al; American College of Cardiology/American Heart Association Task Force on Practice Guidelines. 2014. 2013 ACC/AHA guideline on the treatment of blood cholesterol to reduce atherosclerotic cardiovascular risk in adults: a report of the American College of Cardiology/American Heart Association Task Force on Practice Guidelines. *Circulation.* **129:** S1–S45.

14. Lamon-Fava, S., M. R. Diffenderfer, P. H. R. Barrett, A. Buchsbaum, N. R. Matthan, A. H. Lichtenstein, G. G. Dolnikowski, K. Horvath, B. F. Asztalos, V. Zago, et al. 2007. Effects of different doses of atorvastatin on human apolipoprotein B-100, B-48, and A-I metabolism. *J. Lipid Res.* **48:** 1746–1753.

15. Ooi, E. M. M., P. H. R. Barrett, D. C. Chan, P. J. Nestel, and G. F. Watts. 2008. Dose-dependent effect of rosuvastatin on apolipoprotein B-100 kinetics in the metabolic syndrome. *Atherosclerosis.* **197:** 139–146.

16. Le, N-A., M. R. Diffenderfer, N. Thongtang, E. M. M. Ooi, P. H. R. Barrett, K. V. Horvath, G. G. Dolnikowski, B. F. Asztalos, E. J. Schaefer, and W. V. Brown. 2015. Rosuvastatin enhances the catabolism of LDL apoB-100 in subjects with combined hyperlipidemia in a dose dependent manner. *Lipids.* **50:** 447–458.

17. Karlsson, H., P. Leanderson, C. Tagesson, and M. Lindahl. 2005. Lipoproteomics I: mapping of proteins in low-density lipoprotein using two-dimensional gel electrophoresis and mass spectrometry. *Proteomics.* **5:** 551–565.

18. Karlsson, H., H. Mörtstedt, H. Lindqvist, C. Tagesson, and M. Lindahl. 2009. Protein profiling of low-density lipoprotein from obese subjects. *Proteomics Clin. Appl.* **3:** 663–671.

19. Dashty, M., M. M. Motazacker, J. Levels, M. de Vries, M. Mahmoudi, M. P. Peppelenbosch, and F. Rezaee. 2014. Proteome of human plasma very low-density lipoprotein and low-density lipoprotein exhibits a link with coagulation and lipid metabolism. *Thromb. Haemost.* **111:** 518–530.

20. Melish, J., N-A. Le, H. Ginsberg, D. Steinberg, and W. V. Brown. 1980. Dissociation of apoprotein B and triglyceride production in very low density lipoproteins. *Am. J. Physiol.* **239:** E354–E362.

21. Ginsberg, H. N., N-A. Le, J. Melish, D. Steinberg, and W. V. Brown. 1981. Effect of a high carbohydrate diet on apoprotein-B catabolism in man. *Metabolism.* **30:** 347–353.

22. Cobelli, C., G. Toffolo, D. M. Bier, and R. Nosadini. 1987. Models to interpret kinetic data in stable isotope tracer studies. *Am. J. Physiol.* **253:** E551–E564.

23. Ooi, E. M. M., A. H. Lichtenstein, J. S. Millar, M. R. Diffenderfer, S. Lamon-Fava, H. Rasmussen, F. K. Welty, P. H. R. Barrett, and E. J. Schaefer. 2012. Effects of therapeutic lifestyle change diets high and low in dietary fish-derived FAs on lipoprotein metabolism in middle-aged and elderly subjects. *J. Lipid Res.* **53:** 1958–1967.

24. Beltz, W. F., Y. A. Kesäniemi, B. V. Howard, and S. M. Grundy. 1985. Development of an integrated model for analysis of the kinetics of apolipoprotein B in plasma very low density lipoproteins, intermediate density lipoproteins, and low density lipoproteins. *J. Clin. Invest.* **76:** 575–585.

25. Phair, R. D., M. G. Hammond, J. A. Bowden, M. Fried, W. R. Fisher, and M. Berman. 1975. Preliminary model for human lipoprotein metabolism in hyperlipoproteinemia. *Fed. Proc.* **34:** 2263–2270.

26. Campos, H., B. W. Walsh, H. Judge, and F. M. Sacks. 1997. Effect of estrogen on very low density lipoprotein and low density lipoprotein subclass metabolism in postmenopausal women. *J. Clin. Endocrinol. Metab.* **82:** 3955–3963.

27. Aguilar-Salinas, C. A., P. H. R. Barrett, J. Pulai, X. L. Zhu, and G. Schonfeld. 1997. A familial combined hyperlipidemic kindred with impaired apolipoprotein B catabolism. Kinetics of apolipoprotein B during placebo and pravastatin therapy. *Arterioscler. Thromb. Vasc. Biol.* **17:** 72–82.

28. Zheng, C., C. Khoo, J. Furtado, and F. M. Sacks. 2010. Apolipoprotein C–III and the metabolic basis for hypertriglyceridemia and the dense low-density lipoprotein phenotype. *Circulation.* **121:** 1722–1734.

29. Cohn, J. S., D. A. Wagner, S. D. Cohn, J. S. Millar, and E. J. Schaefer. 1990. Measurement of very low density and low density lipoprotein apolipoprotein (apo) B-100 and high density lipoprotein apo A-I production in human subjects using deuterated leucine. Effect of fasting and feeding. *J. Clin. Invest.* **85:** 804–811.

30. Packard, C. J., T. Demant, J. P. Stewart, D. Bedford, M. J. Caslake, G. Schwertfeger, A. Bedynek, J. Shepherd, and D. Seidel. 2000. Apolipoprotein B metabolism and the distribution of VLDL and LDL subfractions. *J. Lipid Res.* **41:** 305–317.

31. Packard, C. J. 2003. Triacylglycerol-rich lipoproteins and the generation of small, dense low-density lipoprotein. *Biochem. Soc. Trans.* **31:** 1066–1069.

32. Packard, C. J., and J. Shepherd. 1997. Lipoprotein heterogeneity and apolipoprotein B metabolism. *Arterioscler. Thromb. Vasc. Biol.* **17:** 3542–3556.

33. Davidsson, P., J. Hulthe, B. Fagerberg, B-M. Olsson, C. Hallberg, B. Dahllöf, and G. Camejo. 2005. A proteomic study of the apolipoproteins in LDL subclasses in patients with the metabolic syndrome and type 2 diabetes. *J. Lipid Res.* **46:** 1999–2006.

34. Zheng, C. 2014. Updates on apolipoprotein CIII: fulfilling promise as a therapeutic target for hypertriglyceridemia and cardiovascular disease. *Curr. Opin. Lipidol.* **25:** 35–39.

35. Sacks, F. M. 2015. The crucial roles of apolipoproteins E and C–III in apoB lipoprotein metabolism in normolipidemia and hypertriglyceridemia. *Curr. Opin. Lipidol.* **26:** 56–63.

36. McNamara, J. R., D. M. Small, Z. Li, and E. J. Schaefer. 1996. Differences in LDL subspecies involve alterations in lipid composition and conformational changes in apolipoprotein B. *J. Lipid Res.* **37:** 1924–1935.

37. Campos, H., K. S. Arnold, M. E. Balestra, T. L. Innerarity, and R. M. Krauss. 1996. Differences in receptor binding of LDL subfractions. *Arterioscler. Thromb. Vasc. Biol.* **16:** 794–801.

38. Anber, V., B. A. Griffin, M. McConnell, C. J. Packard, and J. Shepherd. 1996. Influence of plasma lipid and LDL-subfraction profile on the interaction between low density lipoprotein with human arterial wall proteoglycans. *Atherosclerosis.* **124:** 261–271.

39. Anber, V., J. S. Millar, M. McConnell, J. Shepherd, and C. J. Packard. 1997. Interaction of very-low-density, intermediate-density, and low-density lipoproteins with human arterial wall proteoglycans. *Arterioscler. Thromb. Vasc. Biol.* **17:** 2507–2514.